MULTIRESOLUTION AUTOMATIC SEGMENTATION OF T1-WEIGHTED BRAIN MR IMAGES

Mahmood Zeydabadi,[1] *Reza A. Zoroofi,*[1] *Hamid Soltanian-Zadeh*[1,2]

[1]Control and Intelligent Processing Center of Excellence, Electrical and Computer Engineering Department, Faculty of Engineering, University of Tehran, Tehran 14395-515, Iran
[2]Image Analysis Lab., Radiology Department, Henry Ford Health System, Detroit, MI 48202, USA

ABSTRACT

Automatic segmentation of brain tissues is crucial to many medical imaging applications. We use a multi-resolution analysis and a power transform to extend the well-known Gaussian mixture model expectation maximization based algorithm for segmentation of white matter, gray matter, and cerebrospinal fluid from T1-weighted magnetic resonance images (MRI) of the brain. Experimental results with near 4000 synthetic and real images are included. The results illustrate that the proposed method outperforms six existing methods.

1. INTRODUCTION

White Matter (WM), Gray Matter (GM), and Cerebrospinal Fluid (CSF) are three main tissues of human brain. With increasing number of brain images, automatic and accurate segmentation of WM, GM, and CSF are needed because manual segmentation is a time consuming and non-repeatable task. Automatic segmentation of the brain soft tissues play a vital role in numerous biomedical imaging applications such as diagnosis, localization of pathology, study of anatomical structures, treatment planning, and computer assisted surgery [1]. Among the medical imaging modalities, magnetic resonance imaging (MRI) has the best soft tissue contrast, although it is not free of additive noise and other imaging artifacts [2].

In this paper, we utilize and extend a parametric model of the image histogram for image segmentation. A statistical model of the image histogram is in the form of a probability density function (pdf) of the pixel intensities. The Gaussian mixture model (GMM) is a well-known statistical model for density estimation due to its tractability and universal approximate capability. If we know the model parameters, we can determine the class that pixel intensity most likely belongs to it through a maximum a posteriori (MAP) procedure. The practical difficulty is that we do not know the model parameters *a priori*. Here, we face with the concept of missing data that the expectation maximization (EM) algorithm [3] is a suitable way to deal with it. The EM algorithm is an iterative procedure to find a maximum likelihood (ML) estimation of the unknown GMM parameters.

In a GMM, we assume that the image histogram is composed of several independent normal distributions. In other words, the conterminous pixels are independent and identically distributed (i.i.d.), but this fundamental assumption causes error in segmentation results due to the presence of noise and other artifacts in MRI. In homogenous regions, the pixel intensities are correlated, although noise and artifacts change them to some extent. Without considering the spatial correlation between such pixels, we cannot segment them properly using the basic GMM. To improve the segmentation results, we propose a multiresolution wavelet based GMM segmentation algorithm to incorporate the spatial correlation between image pixels. Since in real world, not all the images have a normal shape histogram [4], we used a power transform to increase the normality.

The rest of the paper is organized as follows. In Section 2, we review the basic theory. In Section 3, we propose our multiresolution algorithm. Experimental results are given in Section 4 and conclusions in Section 5.

2. THEORY

A mixture model with K >1 components is defined as follows:

$$f(y_j)=\sum_{k=1}^{K}\rho_k f_k(y_j;\theta_k) \qquad \forall \mathrm{y_j}\in\Re^n, n\geq 1 \quad (1)$$

where $\rho_k \in (0,1)$ $(\forall k=1,2,...,K)$, $\sum_{k=1}^{K}\rho_k=1$ are the mixing proportions. For the GMM, each component is a normal *pdf:*

$$f_k(y_j;\theta_k)=\frac{1}{\sqrt{(2\pi)^n \det(\Sigma_k)}} \times \exp\{\frac{-1}{2}(y_j-\mu_k)^T\Sigma_k^{-1}(y_j-\mu_k)\} \quad (2)$$

where $\theta_k = (\mu_k, \Sigma_k)$ is the parameter set of the *k*-th normal *pdf*. Let's define the set of all model parameters as $\Phi = \{\theta_1, \theta_2, ..., \theta_K, \rho_1, \rho_2, ..., \rho_K\}$. To find Φ, we use the EM algorithm. The basic EM algorithm has two steps: expectation step (E-step) and maximization step (M-step). The E-step computes the expected log-likelihood function based on the current estimation of Φ

$$Q(\Phi \mid \Phi^{(t)}) = \sum_{j=1}^{J} \sum_{k=1}^{K} \{\log \rho_k f(y_j; \theta_k)\} f(k; y_j, \Phi^{(t)})$$

where $\Phi^{(t)}$ is the Φ estimation after the *t*-th iteration and

$$f(k; y_j, \Phi^{(t)}) = \frac{\rho_k^{(t)} f(y_j; \theta_k^{(t)})}{\sum_{l=1}^{K} \rho_l^{(t)} f(y_j; \theta_l^{(t)})}. \quad (3)$$

The M-step updates Φ using the data from the E-step and by maximizing the $Q(\Phi \mid \Phi^{(t)})$. This yields an ML estimation of the $\Phi^{(t+1)}$

$$\rho_k^{(t+1)} = \frac{1}{J} \sum_{j=1}^{J} f(k; y_j, \Phi^{(t)}) \quad (4)$$

$$\mu_k^{(t+1)} = \frac{\sum_{j=1}^{J} y_j f(k; y_j, \Phi^{(t)})}{\sum_{j=1}^{J} f(k; y_j, \Phi^{(t)})} \quad (5)$$

$$\Sigma_k^{(t+1)} = \frac{\sum_{j=1}^{J} f(k; y_j, \Phi^{(t)}) \{(y_j - \mu_k^{(t+1)})(y_j - \mu_k^{(t+1)})^T\}}{\sum_{j=1}^{J} f(k; y_j, \Phi^{(t)})} \quad (6)$$

These steps iteratively update the unknown parameters until reaches a stop condition.

3. PROPOSED ALGORITHM

The basic GMM suffers from lack of spatial correlation consideration. Ambroise, et al. [5] proposed to add a penalty term to the log-likelihood function that takes into account the spatial relationship between image pixels through a neighborhood. In this section, we propose a technique to alleviate the lack of spatial correlation consideration using a multi-resolution approach. Multi-resolution analysis (MRA) tends to discover and take into account more image features by inspecting different resolutions of the original image. In addition to intra-scale, by MRA we can extend the pixel relationships into inter-scale mode. Here we use this characteristic to improve the segmentation results of the basic GMM. In MRA, each pixel in a lower resolution is related to at least four pixels in a higher resolution. This forms a parent-child relation that can be used to avoid mistakenly assigning a pixel to a wrong class due to the change that noise or other artifacts cause in its intensity. This inter-scale relationship is justified as follows: when a parent pixel is assigned to a certain class say *k*, the child pixels are more likely to belong to the same class. To take advantages of this relationship, we propose to combine segmentation result of the original image with the one from a lower resolution one. This combination may produce error near the image edges because often the pixels near an edge belong to different tissues. Thus, we should avoid the combination near the edges. We use the Canny edge detector to find the edges in the original and approximate images. The Canny operator works in a multi-stage process. First, the image is smoothed by Gaussian convolution. Then, a simple 2-D first derivative operator (e.g., Roberts Cross) is applied to the smoothed image to highlight regions of the image with high values of the first derivative. Edges give rise to ridges in the gradient magnitude image. The algorithm then tracks along the top of these ridges and sets to zero all pixels that are not actually on the ridge top so as to give a thin line in the output, a process known as non-maximal suppression. The tracking process exhibits hysteresis controlled by two thresholds: *Th1* and *Th2* with *Th1* > *Th2*. Tracking can only begin at a point on a ridge higher than *Th1*. Tracking then continues in both directions out from that point until the height of the ridge falls below *Th2*. This hysteresis helps to ensure that noisy edges are not broken up into multiple edge fragments.

To produce a lower resolution image a good method is to use the 2D-discrete wavelet transform (2D-DWT). To perform this transform, we take first 1D-DWT from all the image rows and then from all the columns of the resultant image. By doing this, we obtain an image with the same size of the original image but composed of four portions (often called LL, LH, HL HH) and contain the different frequencies in horizontal and vertical directions. LL is also named as the approximate image and is a coarser version of the original image.

Another modification we applied to GMM to increase its compatibility with real images is to use the Box-Cox transform [4]. This transforms non-normally distributed data to a set of data that has approximately normal distribution. The Box-Cox transformation is a family of power transformations defined by

$$y_j^{(\lambda)} = \begin{cases} \dfrac{y_j^{\lambda} - 1}{\lambda}, & 0 < \lambda \\ \ln(y_j), & \lambda = 0 \end{cases} \quad (7)$$

where λ is the transformation parameter. After the transformation, $y_j^{(\lambda)}$ is used in place of y_j in (3)-(6). To estimate the λ in M-step the following equation is solved [4].

$$\sum_{j=1}^{J}\left\{\frac{f'(y_j^{(\lambda)})}{f(y_j^{(\lambda)})}\frac{\partial}{\partial\lambda}(y_j^{(\lambda)})+\ln(y_j)\right\}=0 \qquad (8)$$

The proposed multiresolution segmentation algorithm (MRSA) can be summarized as follows:

1. Take the 2D-DWT to obtain the approximate image.
2. Apply the modified EM algorithm to original and approximate images to obtain the segmentations S1 and S2, respectively.
3. Apply the Canny edge detector to original and approximate images to obtain two binary masks that contain the edges of related images.
4. Mask S1 and S2 with their related masks from Step 3 to obtain final segmentation *S* where $S=0.6S1+0.4S2$. The weighting coefficients are found empirically.

4. EXPERIMENTAL RESULTS

To evaluate the performance of proposed method we performed two experiments on near 4000 synthetic and real images. First, we used the simulated images created by Brainweb simulator [6]. This site also provides the ground truth that enabled us to obtain a quantitative assessment of the performance of the algorithm. In the earlier version of the MRI simulator, partial volume effect was not appropriately modeled. The images that we used include different noise levels, RF non-uniformity and also partial volume effect. We considered the following cases:

1. T1-weighted images with 1% to 9% noise levels and no RF non-uniformity.
2. Same as 1 with intensity variations up to 40% for each tissue class (40% RF non-uniformity).

All of the images have the same dimensions, 181*217 and each dataset has 181 slices.

To evaluate performance of the proposed method, we computed the following quality measurements

$$\begin{aligned} Sensitivity &= \frac{TP}{TP+FN}\times 100\% \\ Specificity &= \frac{TN}{TN+FP}\times 100\% \\ Accuracy &= \frac{TN+TP}{TN+TP+FN+FP}\times 100\% \end{aligned} \qquad (9)$$

where TP, FP, TN, and FN are abbreviations for true positive, false positive, true negative, and false negative, respectively. True positive is the set of pixels that both the MRSA algorithm and ground truth assign to the same class. False positive is the set of pixels that the MRSA assign to a class say k, but the ground truth do not assign. True negative is the set of pixels that both the MRSA and ground truth reject to be in class k and false negative is the set of pixels that the MRSA reject to be in class k, but ground truth does not. Fig. 1 shows these measurements for the second set of simulated images. Fig. 2 shows the samples of the simulated images and the segmentation results obtained by the proposed MRSA.

In addition to simulated images, we used real images to evaluate our work. This is a difficult task, because most of the available databases contain only the images without a ground truth or gold standard but fortunately there is a database on the World Wide Web that contains real images with their ground truths. The 20 normal MR brain datasets and their manual segmentations are provided by the center for morphometric analysis at Massachusetts general hospital (MGH) and are available at IBSR [7]. All the images have the same dimensions, 256×256, and each dataset has roughly 64 slices. The ground truth (manual segmentation) contains four classes, WM, GM, CSF, and others that presented by intensity levels 254, 192, 128, and 0, respectively. Performance results from six automatic segmentation methods are also provided at this site. Using the results, it is possible to compare our methods to those reported on the site. In order to perform a meaningful comparison, we use the same performance index. This index is the Tanimoto similarity index

$$I(k)=\frac{n_{a\cap b}(k)}{n_{a\cup b}(k)} \qquad (10)$$

where $n_{a\cap b}(k)$ is the number of pixels classified by both MRSA and ground truth as class k, and $n_{a\cup b}(k)$ denotes the number of pixels classified as class k by either the MRSA or ground truth. Fig. 3 shows the Tanimoto similarity index averaged on the 20 real image sets for the proposed MRSA and six automatic segmentation methods provided by [7]. Fig. 4 shows samples of the real images and the segmentation results of the proposed MRSA. The measurement quality indices (sensitivity, specificity, accuracy) and the Tanimoto similarity index show the superiority of the MRSA. Also, the segmentation results are visually similar to the manual segmentation or the ground truth. All the experiments are done with a P4-1.7MHz PC using the MATLAB 6.5 environment. The average time to segment a 256×256 image is 12 seconds.

5. CONCLUSION

In this paper, we proposed a multiresolution algorithm with a modification in EM algorithm to alleviate the main drawbacks of the basic GMM, i.e., not considering spatial correlation and its incompatibility with the non-normally distributed data. The experimental results with near 4000 synthetic and real images show high performance of the proposed algorithm and its superiority to the existing methods. Local convergence of the EM algorithm is another problem that we intend to deal with in our future work.

REFERENCES

[1] D.L. Pham, C. Xu, J.L. Prince, "A Survey of Current Methods in Medical Image Segmentation," *Technical report, Johns Hopkins University*, Baltimore, January 1998.

[2] Z.P. Liang, P.C. Lauterbur, *Principles of Magnetic Resonance Imaging, A Signal Processing Perspective*, IEEE Press, New York, 2000.

[3] T.K. Moon, "The Expectation Maximization Algorithm," *IEEE Signal Processing Magazine*, pp. 47-60, November 1996.

[4] J.D. Lee, M. Liou, P.E. Cheng, C.C. Chen, "Partition MR Images by Extended EM Segmentation," *Proceedings ICONIP*, vol. 1, pp. 430-435, 2001.

[5] C. Ambroise, G. Govaert, "Spatial Clustering and the EM Algorithm," *Conference Proceedings of International Workshop on Mixtures*, France, pp. 17-2, 1995.

[6] http://www.bic.mni.mcgill.ca/brainweb/

[7] http://www.cma.mgh.harvard.edu/ibsr

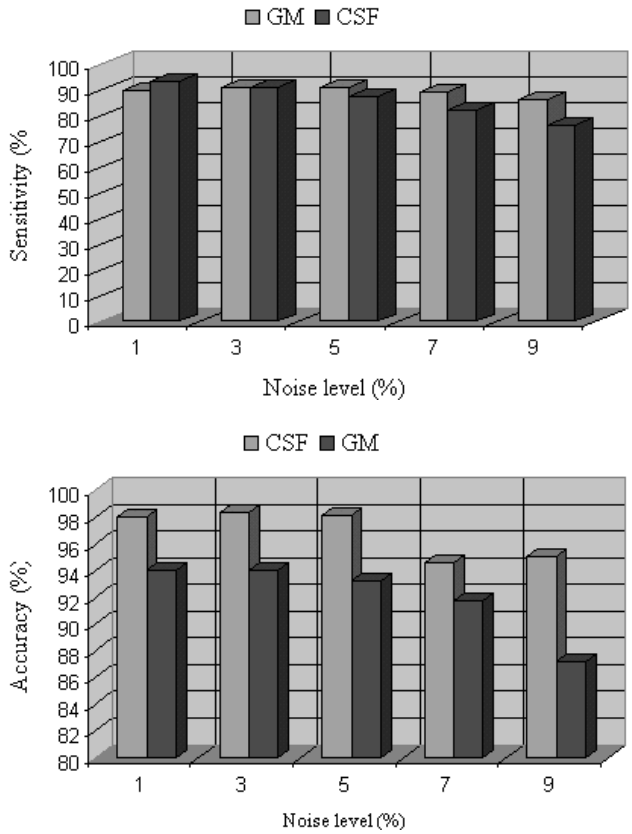

Figure 1. Sensitivity and Accuracy measurement for the second set of simulated images.

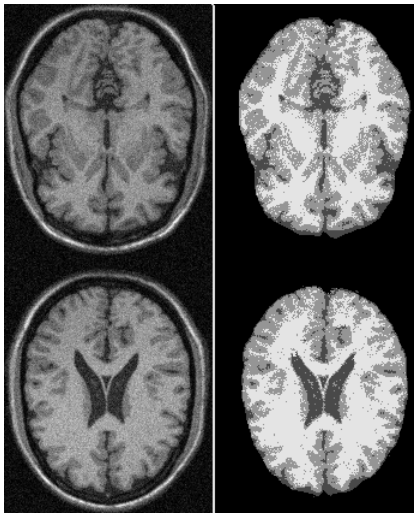

Figure 2. Left column shows sample images from brainweb with 9% noise and 40% RF non-uniformity. Right column shows the MRSA results.

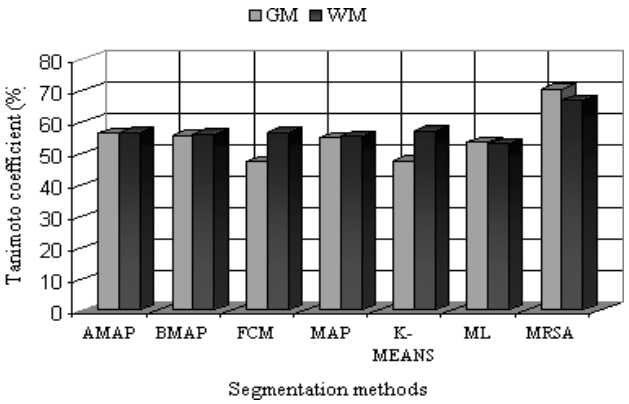

Figure 3. Comparison of average Tanimoto coefficients for the MRSA and six segmentation methods from IBSR [7].

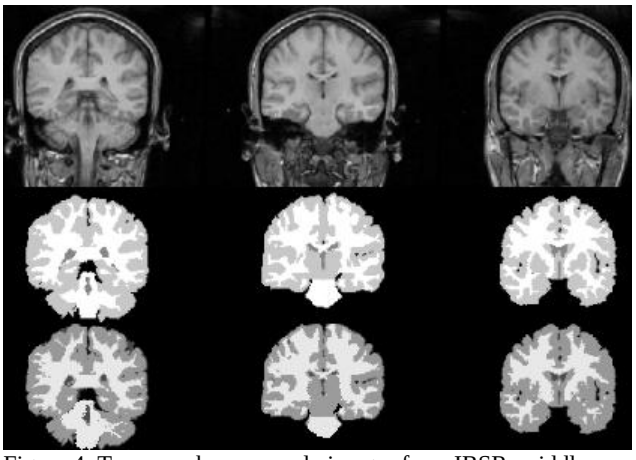

Figure 4. Top row shows sample images from IBSR, middle row shows expert segmentation, and bottom row shows MRSA segmentation. Visual closeness between expert and MRSA segmentation is evident.